Discovery of Small Molecule Integrin $\alpha_v\beta_3$ Antagonists as Novel Anticancer Agents

Raveendra Dayam,[†] Francesca Aiello,[†] Jinxia Deng,[†] Yun Wu,[‡] Antonio Garofalo,[§] Xiaoyuan Chen,*[,‡] and Nouri Neamati*[,†]

Department of Pharmaceutical Sciences, University of Southern California, Los Angeles, California 90033, Molecular Imaging Program at Stanford, Department of Radiology (MIPS) and Bio-X, Stanford University, Stanford, California 94305, and Dipartimento di Scienze Farmaceutiche, Università della Calabria, 87036 Arcavacata di Rende (Cs), Italy

Received December 30, 2005

Integrin $\alpha_v\beta_3$ has been implicated in multiple aspects of tumor progression and metastasis. Many tumors have high expression of $\alpha_v\beta_3$ that correlates with tumor progression. Therefore, $\alpha_v\beta_3$ receptor is an excellent target for drug design and delivery. We have discovered a series of novel $\alpha_v\beta_3$ antagonists utilizing common feature pharmacophore models. Upon validation using a database of known $\alpha_v\beta_3$ receptor antagonists, a highly discriminative pharmacophore model was used as a 3D query. A search of a database of 600 000 compounds using the pharmacophore Hypo5 yielded 832 compounds. On the basis of structural novelty, 29 compounds were tested in $\alpha_v\beta_3$ receptor specific binding assay and four compounds showed excellent binding affinity. A limited SAR analysis on the active compound **26** resulted in the discovery of two compounds with nanomolar to subnanomolar binding affinity. These small-molecule compounds could be conjugated to paclitaxel for selective delivery to $\alpha_v\beta_3$ positive metastatic cancer cells.

Introduction

Integrins, a family of transmembrane adhesion receptors, are principal mediators of cell attachment, migration, differentiation, and survival.[1] Structurally, integrins are heterodimeric receptors that are composed of large extracellular domains, one transmembrane helix, and small intracellular domains for each subunit.[2] These receptors consist of an α- and a β-subunit, which associate noncovalently in defined combinations. To date, 18 α-subunits and eight β-subunits have been identified, which associate selectively to form at least 24 integrins. In addition to their adhesive functions, integrins transduce messages via various signaling pathways and influence proliferation and apoptosis of tumor cells, as well as activated endothelial cells.[3,4] Unique combinations of integrins on the cell surface allows cells to recognize and respond to a variety of extracellular ligands. Integrin $\alpha_v\beta_3$ is a prominent member of the integrin family. It has been implicated in the pathophysiology of malignant tumors where it is required for tumor angiogenesis.[5] It is also highly expressed on both endothelial cells in neovasculature and highly aggressive human carcinomas. Integrin $\alpha_v\beta_3$ mediates adhesion of tumor cells on a variety of extracellular matrix proteins, allowing these cells to migrate during invasion and extravasation.[6,7] In breast cancer, $\alpha_v\beta_3$ characterizes the metastatic phenotype, where it is upregulated in invasive tumors and distant metastases.[8−10] Antagonism of integrin $\alpha_v\beta_3$ is therefore expected to provide a novel approach for the treatment of metastatic and invasive cancers.[11,12] The combination of $\alpha_v\beta_3$ antagonists with conventional treatment modalities could increase the efficacy of metastatic cancer therapy without additional toxicity. The $\alpha_v\beta_3$ receptor binds to a variety of extracellular matrix proteins, including fibrinogen, fibronectin, osteopontin, thrombospondin, and vitronectin, largely through interaction with the Arg-Gly-Asp (RGD[a]) tripeptide sequence.[13,14] Previously, a variety of peptidomimetic small molecule $\alpha_v\beta_3$ antagonists have been identified, some of which are active in disease models such as osteoporosis and skeletal metastatic breast cancer.[12,15−18]

The $\alpha_v\beta_3$ antagonists potently inhibit angiogenesis in a number of animal models, including mouse xenograft and metastases models. Inhibition of $\alpha_v\beta_3$ activity by mAb and cyclic RGD peptides has been shown to induce endothelial apoptosis, and inhibit angiogenesis.[19,20] The $\alpha_v\beta_3$ antagonists can induce apoptosis not only in activated endothelial cells but also in $\alpha_v\beta_3$-positive tumor cells, resulting in a direct cytotoxic effect on tumor cells.[21] Antagonism of $\alpha_v\beta_3$ activity has resulted in decreased tumor growth in breast cancer xenografts and melanoma xenografts.[22,23] Cilengitide, a cyclic RGD peptide in clinical trials for metastatic cancer,[24] has been tested in an aggressive breast cancer model where it was shown that the combination of Cilengitide with radioimmunotherapy remarkably enhanced efficacy and increased apoptosis, compared to single-modality therapy with either agent, without additional toxicity.[25] This suggests a real therapeutic potential of Cilengitide specifically, and $\alpha_v\beta_3$ antagonists in general, in combination anticancer therapy.

The $\alpha_v\beta_3$ receptor also plays a pivotal role in bone resorption. Various studies have indicated that the $\alpha_v\beta_3$ receptor is the most abundant integrin in osteoclasts.[26−29] $\alpha_v\beta_3$ antibodies, RGD peptides, and peptidomimetic antagonists were shown to inhibit bone resorption in vivo without notable adverse affects.[30−34] On the basis of these studies, and results from initial clinical trials, $\alpha_v\beta_3$ antagonists show great promise for the treatment and prevention of osteoporosis.

To identify potent and highly selective structurally diverse small-molecule integrin $\alpha_v\beta_3$ antagonists, we employed three-dimensional (3D) pharmacophore models based on chemical features of a known set of integrin $\alpha_v\beta_3$ antagonists. A subsequent search of a subset of our in-house database of approximately 600 000 small-molecules led to the identification of a series of novel and highly potent $\alpha_v\beta_3$ antagonists.

* Corresponding authors. (N.N.) Phone: 323-442-2341, Fax: 323-442-1390, E-mail: neamati@usc.edu. (X.C.) Phone: 650-725-0950, Fax: 650-736-0234, E-mail: shawchen@stanford.edu.

[†] University of Southern California.

[‡] Stanford University.

[§] Università della Calabria.

[a] Abbreviations: SAR, structure−activity relationship; 3D, three-dimensional; RGD, arginine-glycine-aspartic acid; mAb, monoclonal antibody; GOLD, genetic optimization for ligand docking; MIDAS, metal ion-dependent adhesion site.

10.1021/jm051296s CCC: $33.50
Published on Web 07/01/2006

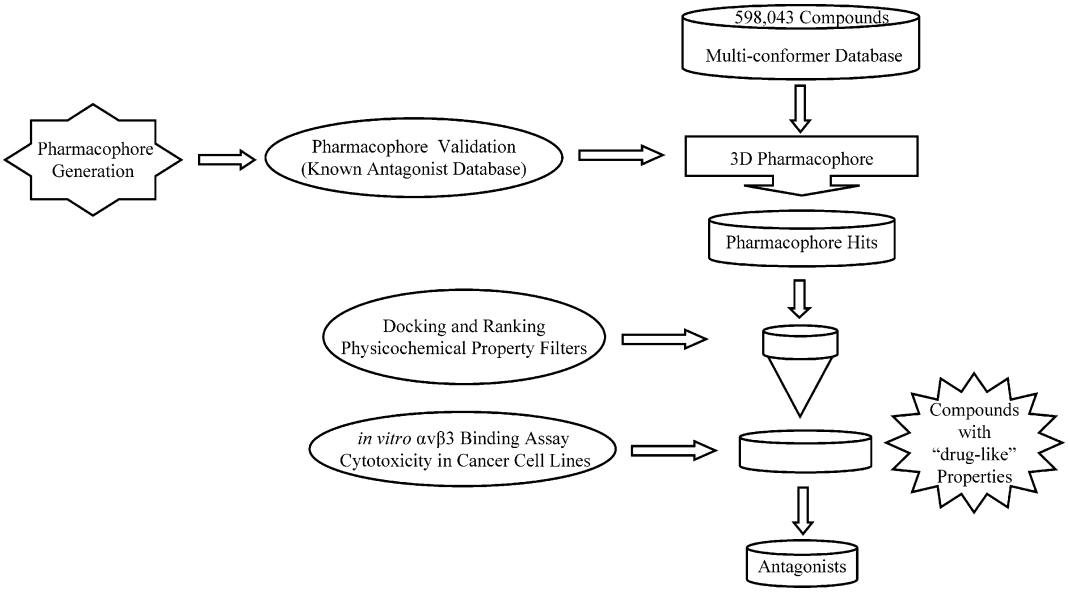

Figure 1. Schematic representation of pharmacophore guided design and discovery of novel $\alpha_v\beta_3$ antagonists

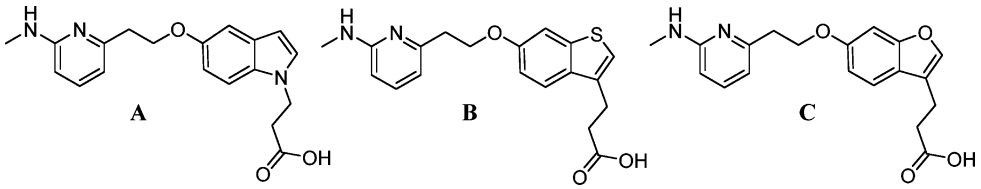

Figure 2. Structures of the training set compounds **A**−**C**.

Interestingly, most of these antagonists showed no cytotoxicity in a panel of cancer cells as a single agent.

Results and Discussion

Design of Integrin $\alpha_v\beta_3$ Antagonists. Previous studies using cyclic RGD peptides suggested that $\alpha_v\beta_3$ recognizes a short overall separation (~6.7 Å) between the key guanidine (Arg) and carboxylic acid (Asp) groups (distance between Cβ atoms of Arg and Asp residues) of the RGD tripeptide sequence.[35,36] Cyclic RGD peptides with a kink in the backbone conformation demonstrated more selectivity toward $\alpha_v\beta_3$ than other integrins.[24] This cyclic RGD peptide−$\alpha_v\beta_3$ interaction model provided the starting point for discovery of a variety of small-molecule peptidomimetic antagonists. The crystal structure of the extracellular segment of $\alpha_v\beta_3$ and its complex with a cyclic RGD peptide has been previously reported.[37,38] We utilized a set of recently reported small-molecule $\alpha_v\beta_3$ antagonists to generate common feature pharmacophore models, which were then validated against a database of 638 known $\alpha_v\beta_3$ antagonists.[39] The validated pharmacophore models were then used as search queries to retrieve molecules with novel structural scaffolds and desired chemical features. Our strategy to identify and design novel $\alpha_v\beta_3$ antagonists is schematically shown in Figure 1.

Generation of Common Feature Pharmacophore Models. Generally, the training set used for generation of common feature pharmacophore models should include compounds with similar activity profiles and active site binding mechanisms, to increase the likelihood that these training compounds have comparable 3D arrangements of chemical features responsible for their biological activity. The HipHop algorithm in the Catalyst software package was applied to a training set consisting of three recently reported antagonists of $\alpha_v\beta_3$ integrin (A, B, and C), each with comparable binding affinities to $\alpha_v\beta_3$ integrin (30 to 49 nM), (Figure 2) to derive common feature pharmacophore models.[39,40] The training set compounds were close analogues and were expected to bind to a similar site on the active site of $\alpha_v\beta_3$ receptor in a similar binding conformation. The pharmacophoric features were selected on the basis of (1) the structural and chemical features of the training set antagonists, (2) the architecture of $\alpha_v\beta_3$ receptor active site, and (3) the critical interactions observed between the cyclic-RGD peptide and prominent $\alpha_v\beta_3$ receptor active residues in the cocrystal structure of the $\alpha_v\beta_3$ receptor complexed with the cyclic-RGD peptide (PDB1L5G).[37] The features considered in the pharmacophore model generation experiment were H-bond donor (HBD), H-bond acceptor (HBA), ring aromatic (HYR), hydrophobic (HYA), and negatively ionizable (NI) feature. HipHop generated 10 five-featured pharmacophore hypotheses. While these hypotheses were similar in their pharmacophoric features, the relative orientation, position, and vector direction of various features were different. Cluster analysis of the 10 hypotheses using a hierarchical complete linkage method available in the Catalyst program produced three clusters. A representative model from each of the three clusters (pharmacophore hypotheses Hypo1, Hypo5, and Hypo9) was selected for further analyses and validation.

Validation of Common Features Pharmacophore Models. As an internal validation the training set compounds **A**−**C** were mapped onto the three pharmacophores. The fit scores and the associated energy of mapped conformations of the training set compounds (Table 1) yielded a lower energy for Hypo5 than Hypo1 or Hypo9 for compounds **A** and **B**, but a relatively high energy for compound **C**. The mapping of Hypo5 onto compound **A**, shown in Figure 3, confirms a good agreement between critical chemical features of this compound and the pharmacophore.

To evaluate the discriminative ability of these pharmacophores in the separation of potent antagonists from inactive

Table 1. Mapping of the Training Set Compounds (**A**−**C**) by Hypo1, Hypo5, and Hypo9

	training set compounds					
	A		B		C	
hypothesis	fit score	conformation energy (kcal/mol)	fit score	conformation energy (kcal/mol)	fit score	conformation energy (kcal/mol)
Hypo1	4.99	19.41	4.98	14.25	4.90	4.42
Hypo5	4.99	6.15	4.94	5.02	4.8	13.54
Hypo9	5.00	16.28	4.87	18.19	4.61	7.83

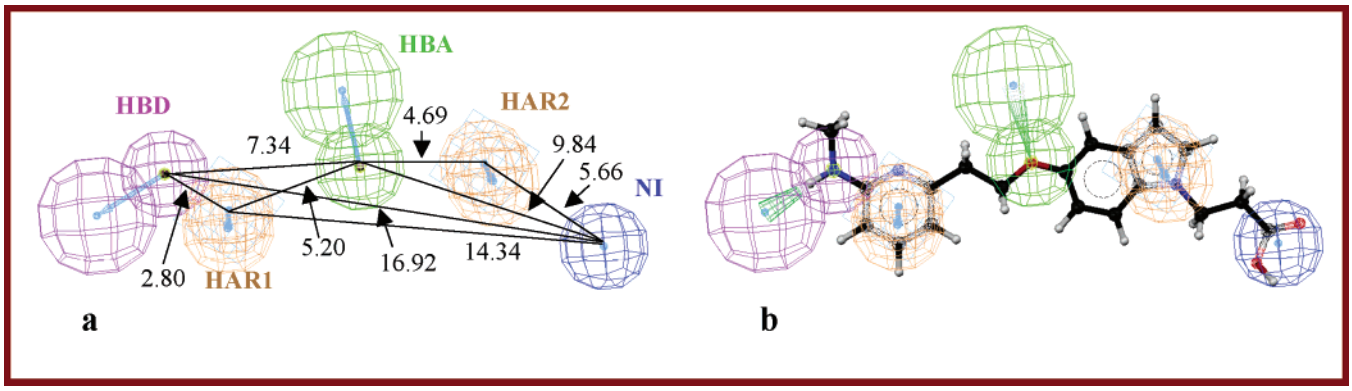

Figure 3. (a) The common feature pharmacophore Hypo5. (b) Hypo5 is mapped onto one of the training set compounds **A**. The important chemical features of compound **A** are mapped by pharmacophoric features of Hypo5. The pharmacophore features are shown as H-bond donor (HBD) in magenta, H-bond acceptor (HBA) in green, hydrophobic aromatic (HAR1−HAR2) in brown, and negatively ionizable feature (NI) in blue. The inter-feature distances are given in Å.

Table 2. Validation of Common Feature Pharmacophore Models Hypo1, Hypo5, and Hypo9 against a Database of Known Integrin $\alpha_v\beta_3$ Antagonists (n = 638)

hypothesis	total hits	active hits	inactive hits	% active
Hypo1	89	51	38	57.3
Hypo5	147	88	59	59.9
Hypo9	182	98	84	53.8

compounds, the three representative pharmacophores were used as 3D queries to search a database of known $\alpha_v\beta_3$ receptor antagonists. This database has a total of 638 compounds with a wide range of activity profiles against the $\alpha_v\beta_3$ receptor. 303 compounds in these database show $\alpha_v\beta_3$ receptor inhibition at IC_{50} values ≤20 nM. These compounds were considered potent $\alpha_v\beta_3$ antagonists. Search results are summarized in Table 2. Hypo5 performed better than the other two pharmacophores retrieving 147 compounds, of which 88 (∼60%) compounds were potent antagonists of $\alpha_v\beta_3$. Hypo9 retrieved more active compounds, but the percent of those considered potent was lower (∼54%) than Hypo5. On the basis of Hypo5's superior ability to select potent antagonists, and the match of Hypo5 to two of the three training set compounds, this pharmacophore was selected for the next step: used as a 3D query to search a subset of our in-house database to retrieve compounds with novel structural scaffolds and desired features.

Database Search and Compound Selection. A search of the NCI2000 database of 238 819 compounds using Hypo5 yielded 684 hits. Of the 684 compounds retrieved by Hypo5, 282 compounds with molecular weight ≤ 500 were considered for further physicochemical property analysis and the remainders were discarded. A search of the Chemical Diversity (ChemDiv, Inc, San Diego, CA) database of 359 224 compounds produced 148 hits. A physicochemical property filter was used to eliminate compounds that did not possess drug-like properties prior to in vitro screening.[41] On the basis of the pharmacophore fit value, calculated physicochemical properties, structural diversity, and sample availability, 8 compounds were obtained from the NCI compound repository and a collection of 21 compounds were purchased from Chemical Diversity for in vitro evaluation.

$\alpha_v\beta_3$ Binding. Receptor binding affinity of all compounds on the surface of nonsmall cell lung cancer NCI-H1975 cells was determined in competitive binding experiments using ^{125}I-labeled echistatin as a radioligand. The results for selected compounds are presented in Table 3. The other compounds tested were inactive in the binding assay. Of the 29 compounds tested, four compounds showed remarkable $\alpha_v\beta_3$ binding affinity (**3** = 52 nM, **26** = 240 nM, **27** = 18 nM, **32** = 605 nM). Two compounds, **3** and **27**, showed a similar range of binding affinity as the training set compounds **A**−**C** (30−49 nM).[39] As observed in the validation analysis, Hypo5 was successful in the retrieval of structurally diverse potent antagonists of $\alpha_v\beta_3$ with nanomolar binding affinity. These compounds represent a novel set of $\alpha_v\beta_3$ antagonists with diverse structural scaffolds. Unlike the training set compounds, the compounds possessed several functional groups of hydrophilic nature. This is an important feature considering the highly electrostatic nature of the RGD peptide binding region of $\alpha_v\beta_3$. The RGD peptide forms strong electrostatic interactions through its two charged ends with $\alpha_v\beta_3$ in the $\alpha_v\beta_3$−cyclic RGD peptide complex crystal structure. Compounds **3**, **27**, and **32** broadly fall into an RGD mimetic antagonist category, since they have a carboxylate group or amine/amide group, at either end that can establish similar electrostatic interactions with $\alpha_v\beta_3$. Additionally, the presence of several hydrophilic functional groups on these compounds favors their interaction with the highly electrostatic region of the RGD binding site of $\alpha_v\beta_3$. Structure−activity studies around the core scaffolds of these two compounds might be an alternative option to further optimize their binding affinity toward $\alpha_v\beta_3$. Possessing unique structural features, compound **26** represents a novel non-RGD mimetic class of $\alpha_v\beta_3$ antagonists. We carried out a limited structure−activity relationship (SAR) analysis on compound **26** by testing compounds **34**−**38** in our binding assay (Table 3). The analogues **34**−**38** were purchased from Chemical Diversity (San Diego, CA) and

Table 3. Novel $\alpha_v\beta_3$ Antagonists Discovered through Pharmacophore-Based Database Searching

compd.	structure	drug-like physicochemical properties[a]						$\alpha_v\beta_3$ binding affinity (nM)
		MW	HBA	HBD	logP	Rb	PSA	
3	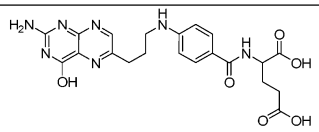	469	13	7	0.7	15	332	52
26	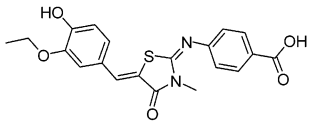	398	7	2	3.6	7	148	240
27	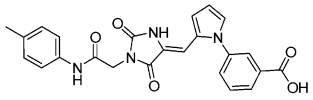	444	9	3	2.7	8	191	18
30	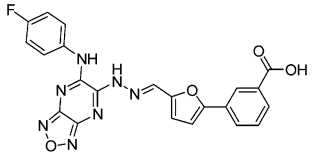	459	11	3	5.3	8	211	>1000
32	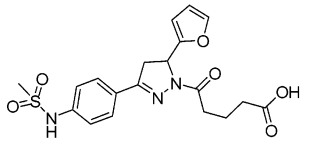	419	9	2	0.7	10	182	605
34[b]	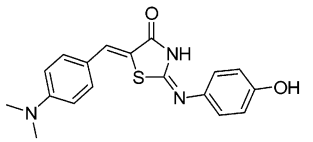	339	5	2	3.67	4	96.1	>1000
35	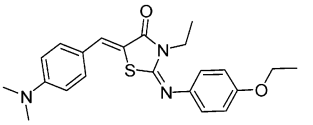	395	5	0	4.82	6	37.9	24
38	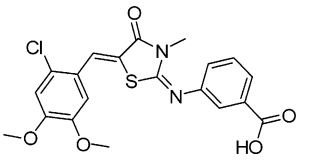	432	7	1	4.22	6	130	0.03

[a] MW: molecular weight, drug-like properties: HBA: number of hydrogen-bond acceptor, HBD: number of hydrogen-bond donor, AlogP98: logarithm of the octanol-water partition coefficient (calculated using Accord for Excell, Accelrys, Inc.), Rb: number of rotatable bond, PSA: 3D-polar surface area (calculated using a Simulations Plus model). [b] Compounds **34**−**38** are analogues of compound **26**.

screened for their $\alpha_v\beta_3$ binding affinity. From this SAR study we discovered two new compounds: **35** with IC_{50} value of 24 nM showed 10-fold higher affinity than the parent compound **26**. Compound **38** with IC_{50} value of 0.03 nM was the most potent and showed 800-fold higher affinity than the parent compound **26**. Compounds **26**, **35**, and **38** deviate structurally from conventional RGD mimetic $\alpha_v\beta_3$ antagonists, suggesting they represent a novel class of non-RGD mimetic antagonists of $\alpha_v\beta_3$ with novel modes of interaction. To our knowledge these compounds are among the most potent $\alpha_v\beta_3$ antagonists described thus far. Together our six compounds represent novel small-molecule $\alpha_v\beta_3$ antagonists, and studies are underway to demonstrate their in vivo efficacy as anticancer agents. Studies are also underway to selectively deliver cytotoxic agents such as paclitaxel to $\alpha_v\beta_3$ integrin overexpressing cancers through covalent conjugation.

Cytotoxicity of Selected Compounds in a Panel of Cancer Cell Lines. Initially, we tested all compounds in two breast cancer cell lines MDA-MB-435 and MCF7 with high and low $\alpha_v\beta_3$ expression as well as in HEY ovarian cancer cell line naturally resistant to cisplatin. Compounds that showed significant inhibition of cell growth at 20 μM (Table 4) were subsequently tested in a panel of five cell lines (Table 5). We observed a remarkable specificity for some of the compounds against these cells. For example, **26** showed more than 60-fold selectivity for MDA-MB-435 cells as compared to the MCF7, NIH3T3, and CRL5908 cells and close to 40-fold selectivity versus the HEY cells. A similar trend, but smaller magnitude,

Table 4. Cytotoxicity of Compounds **1**−**38** in a Panel of Cancer Cell Lines

	% inhibition of cell growth at 20 μM				% inhibition of cell growth at 20 μM		
compd	435[a]	MCF7[b]	HEY[c]	compd	435[a]	MCF7[b]	HEY[c]
1	0	0	14	**21**	26	43	0
2	1	1	0	**22**	25	7	0
3	0	0	0	**23**	9	34	0
4	16	30	0	**24**	9	21	19
5	49	0	0	**25**	26	29	12
6	12	19	0	**26**	94	37	51
7	5	22	0	**27**	0	0	5
8	12	24	6	**28**	32	32	34
9	19	36	0	**29**	14	21	9
10	93	62	73	**30**	71	52	90
11	53	49	0	**31**	21	44	62
14	70	3	0	**32**	0	26	18
15	33	14	14	**34**	65	31	25
17	24	20	5	**35**	26	36	17
18	18	11	0	**36**	16	29	4
19	30	66	6	**37**	3	9	0
20	11	27	0	**38**	0	18	0

[a] 435: MDA-MB-435, breast cancer cell line. [b] MCF7: breast cancer cell lines. [c] HEY: ovarian cancer cell line.

Table 5. Cytotoxicity of Selected Compounds in a Panel of Cancer Cell Lines

	cytotoxicity in a panel of cancer cell-lines (IC_{50}, μM)				
compd	435[a]	MCF-7[b]	NIH3T3[c]	HEY[d]	NCI-H1975[e]
3	>20	>20	>20	>20	>20
10	18 ± 9	>20	-	21 ± 3	-
19	>20	19 ± 4	-	>20	-
26	0.34 ± 0.06	>20	>20	13 ± 8	>20
27	>20	>20	>20	>20	>20
30	8 ± 0.50	19 ± 4	13 ± 3	7 ± 0.42	>20
32	>20	>20	>20	>20	>20
34	2.8 ± 0.01	>20	-	>20	-
35	>20	>20	>20	>20	>20
38	>20	>20	>20	>20	>20

[a] 435: MDA-MB-435, breast cancer cell line. [d] HEY: ovarian cancer cell line. [b] MCF-7: breast cancer cell line. [e] NCI-H1975: lung cancer cell-line. [c] NIH3T3: mouse fibroblast.

was observed with compound **34**. On the other hand **30** showed a profile very similar in MDA-MB-435, HEY, and NIH3T3 cells, but was significantly less active against MCF-7 and NCI-H1975 cells. Interestingly, none of the novel antagonists except **26,** showed notable cytotoxicity, which indicates that the novel antagonists may have utility as noncytotoxic mechanism based anticancer therapeutics. Considering the fact that $\alpha_v\beta_3$ mediates migration, attachment, and apoptosis of cancer cells, the combination of these novel high affinity antagonists with conventional cytotoxic drugs should show improved therapeutic benefits without additional toxicity. Several studies are underway in our laboratory to explore the synergistic effects of these novel antagonists, e.g. **27** and **38** in combination with a number of clinically used cytotoxic agents in a panel of cancer cell lines with low to high levels of $\alpha_v\beta_3$ expression.

Docking Studies. To identify binding orientations of our novel antagonists we have docked compounds **A**, **3**, **26**, **27**, and **38** onto the $\alpha_v\beta_3$ integrin RGD binding region using GOLD.[42] The predicted bound conformations of compounds **A**, **3**, **26**, **27**, and **38** inside the $\alpha_v\beta_3$ RGD binding region are shown in Figure 5a−e. GOLD generated several feasible bound conformations for each compound and ranked them according to their fitness scores. The bound conformation with the most favorable energies was considered the best binding orientation. In the crystal structure of $\alpha_v\beta_3$ receptor complexed with the cyclic RGD peptide, one of the Asp carboxylate oxygens of the cyclic RGD peptide interacts with a Mn^{2+} at MIDAS (metal ion-dependent adhesion site) in the β chain of $\alpha_v\beta_3$ receptor while its Arg guanidinium group interacts with D218 of β chain and D150 of α chain of $\alpha_v\beta_3$ receptor (PDB1L5G). Compounds **A**, **3**, **26**, and **27** established similar binding interactions at their carboxylate end with the Mn^{2+} of MIDAS, as well as several H-bonding interactions with the side chain hydroxyl groups of amino acid residues S121 and S123. In contrast to the bound orientation of the Arg side chain of the cyclic RGD peptide, the amine/amide bearing end of compounds **A**, **3**, **27**, and the hydroxyl bearing phenyl group of **26** occupied a cavity away from D218 of the β chain but close to D150 of the α chain. This cavity is surrounded by amino acid residues Y166, P170, D179, R214, N215, and R216 from β chain and amino acid residues K119, E121, D148, D150, Y178, and R248 from α chain of $\alpha_v\beta_3$. Strikingly, the most potent non-RGD mimetic antagonist **38** adopted a reverse binding orientation and established a set of strong electrostatic interactions with various amino acid residues within the cyclic RGD peptide binding region of $\alpha_v\beta_3$. The schematic presentation of observed key interactions between compounds **A**, **26**, and **38** and various amino acid resides at the $\alpha_v\beta_3$ RGD peptide binding site is shown in Figure 6. The dimethoxy bearing phenyl group of **38** occupied an area close to Mn^{2+} of MIDAS and two methoxy oxygen atoms coordinated to Mn^{2+}. Three H-binding interactions are observed between the methoxy oxygen atoms and the hydroxyl groups of amino acid residues S121 and S123. The carboxylate bearing phenyl group occupied an area surrounded by amino acid residues Y116, P170, D179, R214, and R216 from the β chain and D148, A149, D150, and Y178 from the α chain of $\alpha_v\beta_3$. The carboxylate oxygen atoms formed several strong H-bonding interactions with R216 guanidinium group, the backbone NH of A149 and the hydroxyl group of Y166. A consistent pattern was observed in the predicted binding

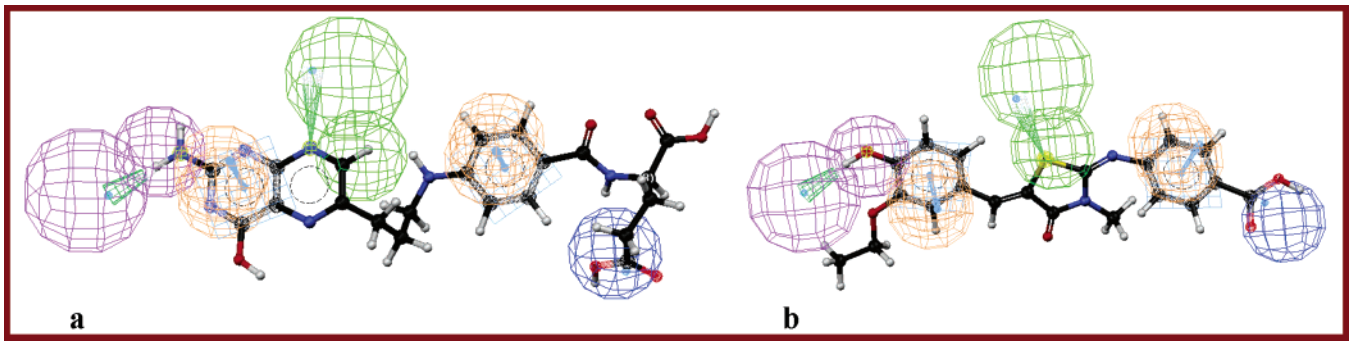

Figure 4. Mapping of Hypo5 onto novel $\alpha_v\beta_3$ receptor antagonists **3** (a) and **26** (b). The pharmacophoric features of Hypo5 are reasonably mapped onto key chemical features of the antagonists. The pharmacophore features are shown as H-bond donor in magenta, H-bond acceptor in green, hydrophobic aromatic in brown, and negatively ionizable feature in blue.

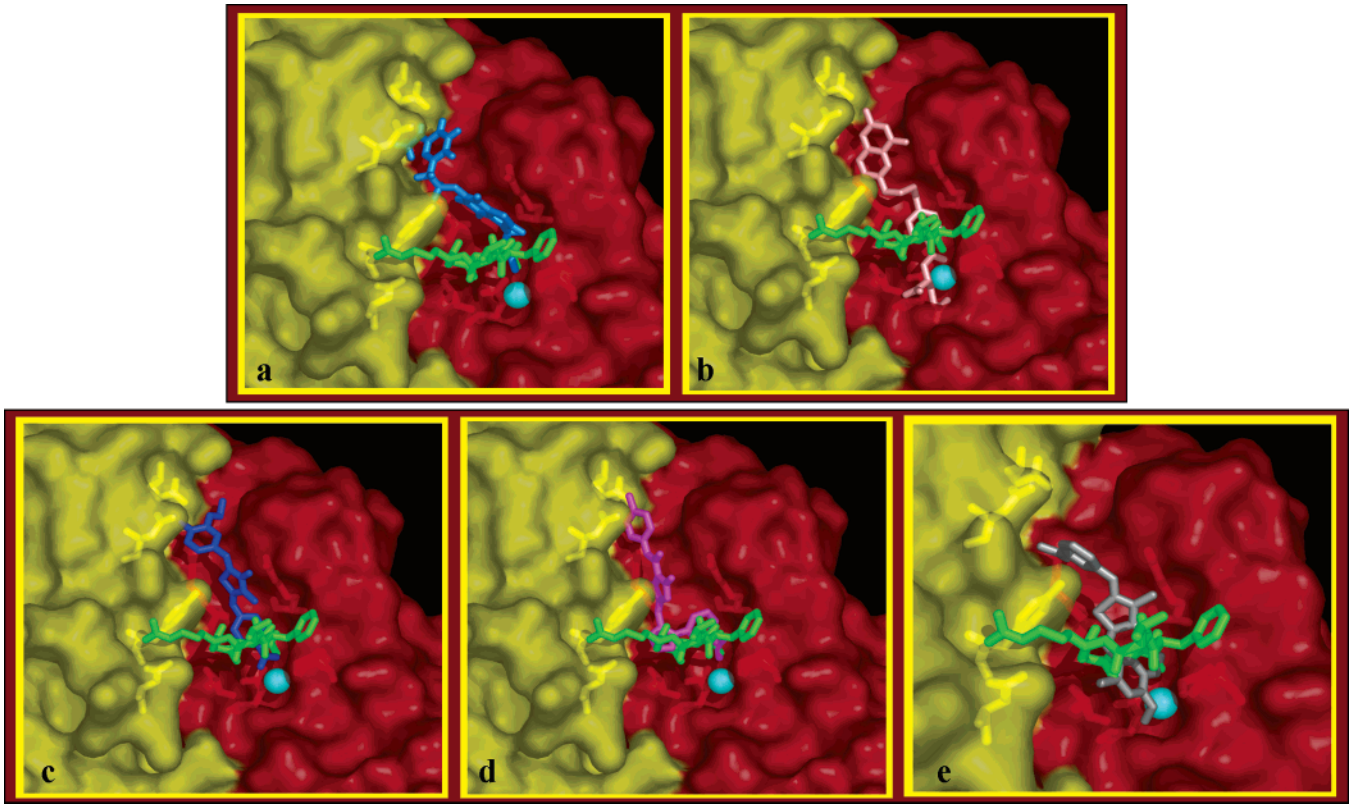

Figure 5. Predicted bound conformation of antagonists **A** (a), **3** (b), **26** (c), **27** (d), and **38** (e) inside the $\alpha_v\beta_3$ RGD peptide binding site. The yellow and red parts represent α and β chains of $\alpha_v\beta_3$ receptor. The prominent active site amino acid residues are shown as stick models on the receptor surface. The green stick model represents the bound orientation of the cyclic-RGD peptide (PDB1L5G). The active site Mn^{2+} (MIDAS) is shown as a cyan sphere.

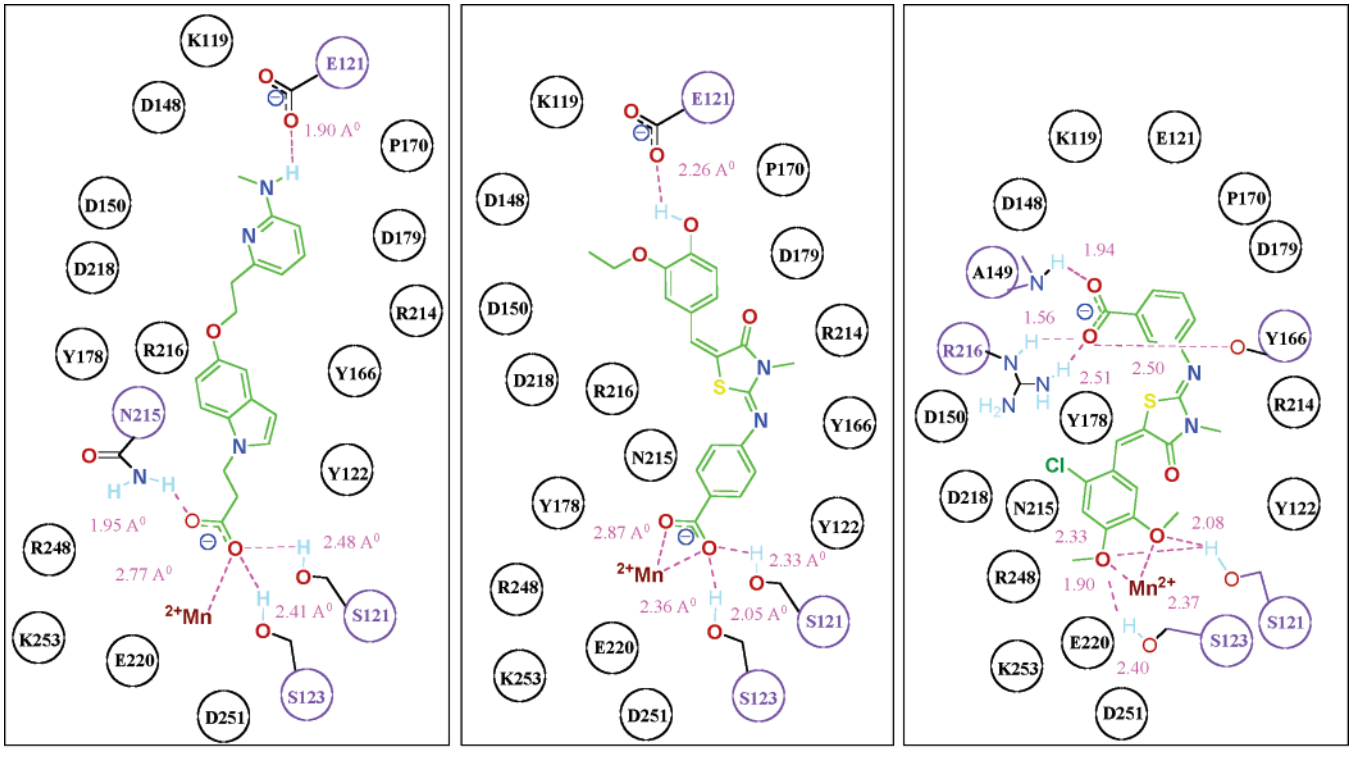

Figure 6. Schematic representation of observed interactions between antagonists **A** (a), **26** (b), and **38** (c) and prominent amino acid residues on $\alpha_v\beta_3$ RGD peptide binding site. The dashed lines represent H-bonding interactions. H-bonding distances are given in Å.

orientations of all the antagonists except the most potent antagonist **38**. The functional groups of these antagonists with similar chemical nature occupied similar areas in the $\alpha_v\beta_3$ RGD peptide binding region and formed similar kinds of interactions with Mn^{2+} and other amino acid residues. This supports the quality of the bound conformations of these antagonists

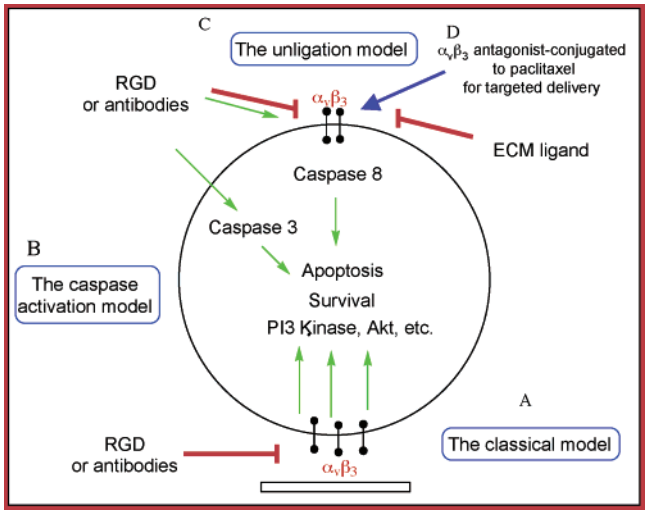

Figure 7. Four models for endothelial apoptosis. (a) The classical model, in which integrin engagement by ligand is necessary to provide survival signals. Inhibitors block ligand binding and thus the survival signals. (b) The caspase activation model, in which RGD peptides directly activate caspases and trigger apoptosis without any involvement of integrins. (c) The unligation model, or "integrin-mediated cell death", in which unligated integrins directly bind and activate caspase-8. ECM ligands block this, but RGD peptides and antibodies binding to the same integrins are not proposed to do so, even though they are known to activate integrins. (d) $\alpha_v\beta_3$ antagonists once conjugated to cytotoxic agents such as paclitaxel can be efficiently delivered to $\alpha_v\beta_3$ positive cancer cells (modified from Richard Hynes, reference 48).

predicted by our docking studies. Several discrepancies were found in the previously predicted binding orientations of RGD mimetic peptidomimetic and non-peptide small-molecule antagonists.[43−47] Previously reported docking studies using non-peptide small-molecule antagonists also predicted very similar binding orientations to the orientation predicted in this study.[43,45] However, docking studies performed on cyclic-RGD analogues and RGD mimetics produced binding orientations similar to the bound conformation of the cyclic RGD in the $\alpha_v\beta_3$−RGD complex crystal structure.[46,47] The observed discrepancies between the predicted binding orientations of our novel antagonists and bound conformation of the cyclic RGD peptide in the $\alpha_v\beta_3$−RGD complex crystal structure may be due to a significant structural difference between the cyclic RGD peptide and these novel antagonists. On the other hand observed discrepancies may also be a result of artifacts in our docking procedure. However, the high binding affinity (800-fold higher than parent **26**) exhibited by our most potent non-RGD mimetic antagonist **38** could be explained by the novel binding interactions found in its predicted binding orientation. In this predicted binding orientation **38** formed seven strong H-bonding interactions and a clear complementarity was found between its functional groups and various amino acid residues around its binding site on $\alpha_v\beta_3$. Further structural studies are warranted to explain the high binding affinity exerted by this non-RGD mimetic antagonist and its interactions with $\alpha_v\beta_3$.

Finally, to explain the recent discrepancy in the field between genetic results with knockout mice and the pharmacological effect with all reported antagonists, we refer the readers to the model by Richard Hynes (Figure 7). This model discusses the reason for β3 integrin knockout mice showing enhanced angiogenesis.[48] It argues that RGD peptides should be in fact referred to as "agonist" instead of "antagonist" to correlate genetic models with the pharmacological models. Although throughout this manuscript we used the word "antagonist" as has been used in most previous reports, we are aware of the possibility that these compounds may be indeed acting as agonists. Regardless of mechanism of action, our compounds are highly potent and very suitable for conjugation to various chemotherapeutic agents for selective delivery to $\alpha_v\beta_3$ positive cells. Therefore, our data are in agreement with the model presented in Figure 7 and our strategy is innovative and warrants further investigation.

Conclusions

We have identified a series of structurally diverse integrin $\alpha_v\beta_3$ antagonists through the pharmacophore screening of a database of small-molecule drug-like compounds. The common features 3D pharmacophore models were generated utilizing a set of known integrin $\alpha_v\beta_3$ antagonists. The validated pharmacophore model successfully retrieved structurally novel compounds with higher potency than the training set compounds that were used to generate the pharmacophores. Furthermore, a limited SAR analysis on one of the potent antagonists resulted in the discovery of highly potent compounds with subnanomlar potency as non-RGD mimetic $\alpha_v\beta_3$ antagonists. These small-molecule antagonists possessing amenable structural scaffolds provide valuable leads for further optimization as potent non-RGD mimetic $\alpha_v\beta_3$ antagonists. We are conjugating three of the potent antagonists with paclitaxel as described in our recent manuscript.[41] Detailed pharmacological properties of these novel agents for targeted delivery to $\alpha_v\beta_3$ positive cancer cells will be presented elsewhere.

Experimental Section

Generation and Validation of Pharmacophore Hypotheses. The structures of the training set compounds (**A**−**C**) were built and thoroughly minimized using Catalyst (Accelrys, Inc.).[40] A set of unique conformations that can explore the accessible conformational flexibility of each compound were generated using Catconf module of Catalyst. The poling algorithm implemented within the Catalyst was used to generate conformations. The poling algorithm promotes high conformational variation and ensures broad coverage of low energy conformational space.[49−51] The common feature pharmacophore hypotheses were generated using the HipHop algorithm of Catalyst. HipHop generates 10 pharmacophore models with its default settings. HipHop takes a collection of conformational models of the training set molecules and a selection of chemical features, and it identifies configurations of features common to the training set molecules. Compound **A** considered as a principle compound in the pharmacophore hypotheses generation experiment. On the basis of structural and chemical features of the training set compounds and the $\alpha_v\beta_3$ active site features, a set of pharmacophoric features were selected in the beginning of the pharmacophore generation experiment. A searchable multiconformer database of the known $\alpha_v\beta_3$ antagonists was generated using Catalyst database server. These database was used to validate the pharmacophore models.

Docking Studies. Docking was performed using version 1.2 of the GOLD program (Genetic Optimization for Ligand Docking).[42] GOLD is an automated docking program that uses genetic algorithm to explore the ligand conformational flexibility with partial flexibility of the active site.[52] The algorithm was tested on a dataset of over 300 complexes extracted from the Brookhaven Protein DataBank. GOLD succeeded in more than 70% cases in reproducing the experimental bound conformation of the ligand.[53] GOLD requires a user defined binding site. It searches for a cavity within the defined area and considers all the solvent accessible atoms in the defined area as active site atoms. Appropriate protonation states were assigned for the acidic and basic amino acid residues. All the water molecules present in the receptor were removed, and hydrogen

atoms were added to the integrin $\alpha_v\beta_3$ receptor. All conformers of each molecule were docked onto the $\alpha_v\beta_3$ receptor active site. At the end of each run GOLD separates and ranks all the generated bound conformations based on the fitness score and root-mean-square distances (RMSD). All docking runs were carried out using standard default settings with a population size of 100, a maximum number of 100 000 operations, and a mutation and crossover rate of 95. The fitness function that is implemented in GOLD consists of H-bonding, complex energy and the ligand internal energy terms. The docking studies were performed on a 24-CPU Silicon Graphics Onyx workstation.

Cell Culture. Human breast cancer cells (MCF-7, $\alpha_v\beta_3$ -, overexpressed wild-type p53, ER+; MDA-MB 468, p53 mutant, ER+; and MDA-MB-435, $\alpha_v\beta_3$+, p53 mutant, ER-) and non-small cell lung cancer cells H1975 were obtained from the American Type Cell Culture (Rockville, MD Q4). The HEY human ovarian carcinoma cell line naturally resistant to cisplatin (CDDP) was kindly provided by Dr. Dubeau (University of Southern California Norris Cancer Center). Cells were maintained as monolayer cultures in RPMI 1640 supplemented with 10% fetal bovine serum (Gemini-Bioproducts, Woodland, CA) and 2 mmol/L L-glutamine at 37 °C in a humidified atmosphere of 5% CO_2. To remove the adherent cells from the flask for passaging and counting, cells were washed with PBS without calcium or magnesium, incubated with a small volume of 0.25% trypsin−EDTA solution (Sigma, St. Louis, MO) for 5 to 10 min, and washed with culture medium and centrifuged. All experiments were done using cells in exponential cell growth.

Drugs. A 10 mM stock solution of all compounds were prepared in DMSO and stored at −20 °C. Further dilutions were freshly made in PBS.

Receptor Binding Assay. Binding affinity of all compounds on the surface of NCI-H1975 cells was determined in competitive binding experiments using ^{125}I-labeled echistatin as radioligand as described in the literature with modifications.[41] In brief, NCI-H1975 cells were harvested, washed twice with PBS, and resuspended (2×10^6 cells/mL) in binding buffer (20 mM Tris, pH 7.4, 150 mM NaCl, 2 mM $CaCl_2$, 1 mM $MgCl_2$, 1 mM $MnCl_2$, 0.1% BSA). A 96-well multiscreen DV plate (filter pore size: 0.65 μm, Millipore, Billerica, MA) was incubated with ^{125}I-echistatin (50 000 cpm/well) in the presence of increasing concentrations of $\alpha_v\beta_3$ antagonists. The total incubation volume was adjusted to 200 μL. After the cells were incubated for 3 h at room temperature, and the plate was filtered through multiscreen vacuum manifold and washed twice with cold binding buffer. The hydrophilic PVDF filters were collected, and the radioactivity was determined using NaI(Tl) gamma counter (Packard, Meriden, CT). The best-fit IC_{50} values were calculated by fitting the data by nonlinear regression using GraphPad Prism (GraphPad Software, Inc., San Diego, CA). Experiments were carried out with triplicate samples.

Cytotoxicity Assay. Cytotoxicity was assessed by 3-(4,5-dimethylthiazol-2-yl)-2,5-diphenyltetrazolium bromide (MTT) assay as previously described.[41,54] Briefly, cells were seeded in 96-well microtiter plates and allowed to attach. Cells were subsequently treated with a continuous exposure to the corresponding drug for 72 h. An MTT solution (at a final concentration of 0.5 mg/mL) was added to each well, and cells were incubated for 4 h at 37 °C. After removal of the medium, DMSO was added and the absorbance was read at 570 nm. All assays were done in triplicate. The IC_{50} was then determined for each drug from a plot of log(drug concentration) versus percentage of cell kill.

Acknowledgment. This study was supported in part by funds from Gustavus and Louise Pfeiffer Research Foundation to Nouri Neamati. We thank Drs. Jonathan Buckley and Burkhard Jansen for their comments throughout this study.

Supporting Information Available: Structures of all the inactive compounds. This material is available free of charge via the Internet at http://pubs.acs.org.

References

(1) Danen, E. H., Integrins: regulators of tissue function and cancer progression. *Curr. Pharm. Des.* **2005**, *11* (7), 881−91.
(2) Humphries, M. J., Integrin structure. *Biochem. Soc. Trans.* **2000**, *28* (4), 311−39.
(3) Martin, K. H.; Slack, J. K.; Boerner, S. A.; Martin, C. C.; Parsons, J. T., Integrin connections map: to infinity and beyond. *Science* **2002**, *296* (5573), 1652−3.
(4) Aplin, A. E.; Howe, A. K.; Juliano, R. L., Cell adhesion molecules, signal transduction and cell growth. *Curr. Opin. Cell Biol.* **1999**, *11* (6), 737−44.
(5) Brooks, P. C.; Clark, R. A.; Cheresh, D. A., Requirement of vascular integrin alpha v beta 3 for angiogenesis. *Science* **1994**, *264* (5158), 569−71.
(6) Hood, J. D.; Cheresh, D. A., Role of integrins in cell invasion and migration. *Nat. Rev. Cancer* **2002**, *2* (2), 91−100.
(7) Felding-Habermann, B., Integrin adhesion receptors in tumor metastasis. *Clin. Exp. Metastasis* **2003**, *20* (3), 203−13.
(8) Natali, P. G.; Hamby, C. V.; Felding-Habermann, B.; Liang, B.; Nicotra, M. R.; Di Filippo, F.; Giannarelli, D.; Temponi, M.; Ferrone, S., Clinical significance of alpha(v)beta3 integrin and intercellular adhesion molecule-1 expression in cutaneous malignant melanoma lesions. *Cancer Res.* **1997**, *57* (8), 1554−60.
(9) Felding-Habermann, B.; O'Toole, T. E.; Smith, J. W.; Fransvea, E.; Ruggeri, Z. M.; Ginsberg, M. H.; Hughes, P. E.; Pampori, N.; Shattil, S. J.; Saven, A.; Mueller, B. M., Integrin activation controls metastasis in human breast cancer. *Proc. Natl. Acad. Sci. U.S.A.* **2001**, *98*, (4), 1853−8.
(10) Pecheur, I.; Peyruchaud, O.; Serre, C. M.; Guglielmi, J.; Voland, C.; Bourre, F.; Margue, C.; Cohen-Solal, M.; Buffet, A.; Kieffer, N.; Clezardin, P., Integrin alpha(v)beta3 expression confers on tumor cells a greater propensity to metastasize to bone. *FASEB J.* **2002**, *16* (10), 1266−8.
(11) Kumar, C. C.; Armstrong, L.; Yin, Z.; Malkowski, M.; Maxwell, E.; Ling, H.; Yaremko, B.; Liu, M.; Varner, J.; Smith, E. M.; Neustadt, B.; Nechuta, T., Targeting integrins alpha v beta 3 and alpha v beta 5 for blocking tumor-induced angiogenesis. *Adv. Exp. Med. Biol.* **2000**, *476*, 169−80.
(12) Shannon, K. E.; Keene, J. L.; Settle, S. L.; Duffin, T. D.; Nickols, M. A.; Westlin, M.; Schroeter, S.; Ruminski, P. G.; Griggs, D. W., Anti-metastatic properties of RGD-peptidomimetic agents S137 and S247. *Clin. Exp. Metastasis* **2004**, *21* (2), 129−38.
(13) Ruoslahti, E.; Pierschbacher, M. D., Arg-Gly-Asp: a versatile cell recognition signal. *Cell* **1986**, *44* (4), 517−8.
(14) Hynes, R. O., Integrins: versatility, modulation, and signaling in cell adhesion. *Cell* **1992**, *69* (1), 11−25.
(15) Kerr, J. S.; Wexler, R. S.; Mousa, S. A.; Robinson, C. S.; Wexler, E. J.; Mohamed, S.; Voss, M. E.; Devenny, J. J.; Czerniak, P. M.; Gudzelak, A., Jr.; Slee, A. M., Novel small molecule alpha v integrin antagonists: comparative anti-cancer efficacy with known angiogenesis inhibitors. *Anticancer Res.* **1999**, *19* (2A), 959−68.
(16) Lark, M. W.; Stroup, G. B.; Hwang, S. M.; James, I. E.; Rieman, D. J.; Drake, F. H.; Bradbeer, J. N.; Mathur, A.; Erhard, K. F.; Newlander, K. A.; Ross, S. T.; Salyers, K. L.; Smith, B. R.; Miller, W. H.; Huffman, W. F.; Gowen, M., Design and characterization of orally active Arg-Gly-Asp peptidomimetic vitronectin receptor antagonist SB 265123 for prevention of bone loss in osteoporosis. *J. Pharmacol. Exp. Ther.* **1999**, *291* (2), 612−7.
(17) Reinmuth, N.; Liu, W.; Ahmad, S. A.; Fan, F.; Stoeltzing, O.; Parikh, A. A.; Bucana, C. D.; Gallick, G. E.; Nickols, M. A.; Westlin, W. F.; Ellis, L. M., Alphavbeta3 integrin antagonist S247 decreases colon cancer metastasis and angiogenesis and improves survival in mice. *Cancer Res* **2003**, *63* (9), 2079−87.
(18) Harms, J. F.; Welch, D. R.; Samant, R. S.; Shevde, L. A.; Miele, M. E.; Babu, G. R.; Goldberg, S. F.; Gilman, V. R.; Sosnowski, D. M.; Campo, D. A.; Gay, C. V.; Budgeon, L. R.; Mercer, R.; Jewell, J.; Mastro, A. M.; Donahue, H. J.; Erin, N.; Debies, M. T.; Meehan, W. J.; Jones, A. L.; Mbalaviele, G.; Nickols, A.; Christensen, N. D.; Melly, R.; Beck, L. N.; Kent, J.; Rader, R. K.; Kotyk, J. J.; Pagel, M. D.; Westlin, W. F.; Griggs, D. W., A small molecule antagonist of the alpha(v)beta3 integrin suppresses MDA-MB-435 skeletal metastasis. *Clin. Exp. Metastasis* **2004**, *21* (2), 119−28.
(19) Brooks, P. C.; Stromblad, S.; Klemke, R.; Visscher, D.; Sarkar, F. H.; Cheresh, D. A., Antiintegrin alpha v beta 3 blocks human breast cancer growth and angiogenesis in human skin. *J. Clin. Invest.* **1995**, *96* (4), 1815−22.
(20) Brooks, P. C.; Montgomery, A. M.; Rosenfeld, M.; Reisfeld, R. A.; Hu, T.; Klier, G.; Cheresh, D. A., Integrin alpha v beta 3 antagonists promote tumor regression by inducing apoptosis of angiogenic blood vessels. *Cell* **1994**, *79* (7), 1157−64.

(21) Taga, T.; Suzuki, A.; Gonzalez-Gomez, I.; Gilles, F. H.; Stins, M.; Shimada, H.; Barsky, L.; Weinberg, K. I.; Laug, W. E., alpha v-Integrin antagonist EMD 121974 induces apoptosis in brain tumor cells growing on vitronectin and tenascin. *Int. J. Cancer* **2002**, *98*, (5), 690−7.
(22) Mitjans, F.; Meyer, T.; Fittschen, C.; Goodman, S.; Jonczyk, A.; Marshall, J. F.; Reyes, G.; Piulats, J., In vivo therapy of malignant melanoma by means of antagonists of alphav integrins. *Int. J. Cancer* **2000**, *87*, (5), 716−23.
(23) Allman, R.; Cowburn, P.; Mason, M., In vitro and in vivo effects of a cyclic peptide with affinity for the alpha(nu)beta3 integrin in human melanoma cells. *Eur. J. Cancer* **2000**, *36* (3), 410−22.
(24) Dechantsreiter, M. A.; Planker, E.; Matha, B.; Lohof, E.; Holzemann, G.; Jonczyk, A.; Goodman, S. L.; Kessler, H., N.-Methylated cyclic RGD peptides as highly active and selective alpha(V)beta(3) integrin antagonists. *J. Med. Chem.* **1999**, *42* 2, (16), 3033−40.
(25) Burke, P. A.; DeNardo, S. J.; Miers, L. A.; Lamborn, K. R.; Matzku, S.; DeNardo, G. L., Cilengitide targeting of alpha(v)beta(3) integrin receptor synergizes with radioimmunotherapy to increase efficacy and apoptosis in breast cancer xenografts. *Cancer Res.* **2002**, *62* (15), 4263−72.
(26) Rodan, S. B.; Rodan, G. A., Integrin function in osteoclasts. *J. Endocrinol.* **1997**, *154* Suppl, S47−56.
(27) Nakamura, I.; Pilkington, M. F.; Lakkakorpi, P. T.; Lipfert, L.; Sims, S. M.; Dixon, S. J.; Rodan, G. A.; Duong, L. T., Role of alpha(v)-beta(3) integrin in osteoclast migration and formation of the sealing zone. *J Cell Sci.* **1999**, *112* (Pt 22), 3985−93.
(28) Duong, L. T.; Rodan, G. A., The role of integrins in osteoclast function. *J Bone Miner. Metab.* **1999**, *17*, (1), 1−6.
(29) Teitelbaum, S. L., Bone resorption by osteoclasts. *Science* **2000**, *289* (5484), 1504−8.
(30) Fisher, J. E.; Caulfield, M. P.; Sato, M.; Quartuccio, H. A.; Gould, R. J.; Garsky, V. M.; Rodan, G. A.; Rosenblatt, M., Inhibition of osteoclastic bone resorption in vivo by echistatin, an "arginyl-glycyl-aspartyl" (RGD)-containing protein. *Endocrinology* **1993**, *132* (3), 1411−3.
(31) Engleman, V. W.; Nickols, G. A.; Ross, F. P.; Horton, M. A.; Griggs, D. W.; Settle, S. L.; Ruminski, P. G.; Teitelbaum, S. L., A peptidomimetic antagonist of the alpha(v)beta3 integrin inhibits bone resorption in vitro and prevents osteoporosis in vivo. *J. Clin. Invest.* **1997**, *99* (9), 2284−92.
(32) Yamamoto, M.; Fisher, J. E.; Gentile, M.; Seedor, J. G.; Leu, C. T.; Rodan, S. B.; Rodan, G. A., The integrin ligand echistatin prevents bone loss in ovariectomized mice and rats. *Endocrinology* **1998**, *139* (3), 1411−9.
(33) Hutchinson, J. H.; Halczenko, W.; Brashear, K. M.; Breslin, M. J.; Coleman, P. J.; Duong le, T.; Fernandez-Metzler, C.; Gentile, M. A.; Fisher, J. E.; Hartman, G. D.; Huff, J. R.; Kimmel, D. B.; Leu, C. T.; Meissner, R. S.; Merkle, K.; Nagy, R.; Pennypacker, B.; Perkins, J. J.; Prueksaritanont, T.; Rodan, G. A.; Varga, S. L.; Wesolowski, G. A.; Zartman, A. E.; Rodan, S. B.; Duggan, M. E., Nonpeptide alphavbeta3 antagonists. 8. In vitro and in vivo evaluation of a potent alphavbeta3 antagonist for the prevention and treatment of osteoporosis. *J. Med. Chem.* **2003**, *46* (22), 4790−8.
(34) Murphy, M. G.; Cerchio, K.; Stoch, S. A.; Gottesdiener, K.; Wu, M.; Recker, R., Effect of L-000845704, an alphaVbeta3 integrin antagonist, on markers of bone turnover and bone mineral density in postmenopausal osteoporotic women. *J. Clin. Endocrinol. Metab.* **2005**, *90* (4), 2022−8.
(35) Pfaff, M.; Tangemann, K.; Muller, B.; Gurrath, M.; Muller, G.; Kessler, H.; Timpl, R.; Engel, J., Selective recognition of cyclic RGD peptides of NMR defined conformation by alpha IIb beta 3, alpha V beta 3, and alpha 5 beta 1 integrins. *J. Biol. Chem.* **1994**, *269* (32), 20233−8.
(36) Burgess, K.; Lim, D.; Mousa, S. A., Synthesis and solution conformation of cyclo[RGDRGD]: a cyclic peptide with selectivity for the alpha V beta 3 receptor. *J. Med. Chem.* **1996**, *39*, (22), 4520−6.
(37) Xiong, J. P.; Stehle, T.; Zhang, R.; Joachimiak, A.; Frech, M.; Goodman, S. L.; Arnaout, M. A., Crystal structure of the extracellular segment of integrin alpha Vbeta3 in complex with an Arg-Gly-Asp ligand. *Science* **2002**, *296* (5565), 151−5.
(38) Xiong, J. P.; Stehle, T.; Diefenbach, B.; Zhang, R.; Dunker, R.; Scott, D. L.; Joachimiak, A.; Goodman, S. L.; Arnaout, M. A., Crystal structure of the extracellular segment of integrin alpha Vbeta3. *Science* **2001**, *294* (5541), 339−45.
(39) Marugan, J. J.; Manthey, C.; Anaclerio, B.; Lafrance, L.; Lu, T.; Markotan, T.; Leonard, K. A.; Crysler, C.; Eisennagel, S.; Dasgupta, M.; Tomczuk, B., Design, synthesis, and biological evaluation of novel potent and selective alphavbeta3/alphavbeta5 integrin dual inhibitors with improved bioavailability. Selection of the molecular core. *J. Med. Chem.* **2005**, *48* (4), 926−34.
(40) *Catalyst 4.9*, Accelrys Inc: San Diego, USA, 2004.
(41) Chen, X.; Plasencia, C.; Hou, Y.; Neamati, N., Synthesis and biological evaluation of dimeric RGD peptide-paclitaxel conjugate as a model for integrin-targeted drug delivery. *J. Med. Chem.* **2005**, *48* (4), 1098−106.
(42) *GOLD 1.2*, CCDC: Cambridge, UK., 2002.
(43) Gottschalk, K. E.; Gunther, R.; Kessler, H., A three-state mechanism of integrin activation and signal transduction for integrin alpha(v)-beta(3). *Chembiochem* **2002**, *3* (5), 470−3.
(44) Gottschalk, K. E.; Kessler, H., The structures of integrins and integrin-ligand complexes: implications for drug design and signal transduction. *Angew. Chem., Int. Ed.* **2002**, *41* (20), 3767−74.
(45) Feuston, B. P.; Culberson, J. C.; Duggan, M. E.; Hartman, G. D.; Leu, C. T.; Rodan, S. B., Binding model for nonpeptide antagonists of alpha(v)beta(3) integrin. *J. Med. Chem.* **2002**, *45* (26), 5640−8.
(46) Marinelli, L.; Lavecchia, A.; Gottschalk, K. E.; Novellino, E.; Kessler, H., Docking studies on alphavbeta3 integrin ligands: pharmacophore refinement and implications for drug design. *J. Med. Chem.* **2003**, *46* (21), 4393−404.
(47) Moitessier, N.; Henry, C.; Maigret, B.; Chapleur, Y., Combining pharmacophore search, automated docking, and molecular dynamics simulations as a novel strategy for flexible docking. Proof of concept: docking of arginine-glycine-aspartic acid-like compounds into the alphavbeta3 binding site. *J. Med. Chem.* **2004**, *47* (17), 4178−87.
(48) Hynes, R. O., A reevaluation of integrins as regulators of angiogenesis. *Nat. Med.* **2002**, *8*, (9), 918−21.
(49) Smellie, A.; Kahn, S. D.; Teig, S. L., Analysis of Conformational Coverage 0.1. Validation and Estimation of Coverage. *J. Chem. Inf. Comput. Sci.* **1995**, *35* (2), 285−294.
(50) Smellie, A.; Kahn, S. D.; Teig, S. L., Analysis of Conformational Coverage 0.2. Application of Conformational Models. *J. Chem. Inf. Comput. Sci.* **1995**, *35* (2), 295−304.
(51) Smellie, A.; Teig, S. L.; Towbin, P., Poling − Promoting Conformational Variation. *J. Comput. Chem.* **1995**, *16* (2), 171−187.
(52) Jones, G.; Willett, P.; Glen, R. C.; Leach, A. R.; Taylor, R., Development and validation of a genetic algorithm for flexible docking. *J. Mol. Biol.* **1997**, *267* (3) 727−48.
(53) Nissink, J. W.; Murray, C.; Hartshorn, M.; Verdonk, M. L.; Cole, J. C.; Taylor, R., A new test set for validating predictions of protein−ligand interaction. *Proteins* **2002**, *49* (4), 457−71.
(54) Plasencia, C.; Dayam, R.; Wang, Q.; Pinski, J.; Burke, T. R., Jr.; Quinn, D. I.; Neamati, N. Discovery and preclinical evaluation of a novel class of small-molecule compounds in hormone-dependent and -independent cancer cell lines. *Mol. Cancer Ther.* **2005**, *4* (7), 1105−13.

JM051296S